

# 129 STRUCTURE OF THE FUKUOKA TORNADO OBSERVED BY DIFFERENT RADARS

Tetsuya Kobayashi \*

Hydrospheric Atmospheric Research Center, Nagoya University, Aichi, Japan

Koji Sassa

Kochi University, Kochi, Japan

Hiroshi Uyeda

Hydrospheric Atmospheric Research Center, Nagoya University, Aichi, Japan

## 1. INTRODUCTION

On the morning of 21 August 2011, a tornado struck the downtown area of Fukuoka City, western Japan. In this paper, we refer to this event as 'the Fukuoka tornado'. This tornado was classified as F1 on the Fujita scale, and more than 20 buildings were destroyed, but fortunately there were few casualties. Video of the tornado showed that it possessed a multiple-vortex structure, which will be described later. Multiple-vortex type tornadoes are rare in Japan, as are detailed radar observations of tornadoes. However, Inoue et al. (2011) analyzed the detailed temporal evolution of four low-level mesocyclones using high-resolution Doppler radar datasets, which were obtained at an interval of 30 seconds, and discussed their generation and development processes. Niino et al. (1993) described an example of a storm similar to a typical supercell storm in Japan, and Kobayashi et al. (1996) found a distinct cascading-scale structure consisting of mesocyclone, mesocyclone, and funnel cloud in a typical supercell tornado. Suzuki et al. (2000) investigated a mini supercell (which noted by McCaul 1987) associated with a typhoon, and noted that a supercell generated in a moist environment had several characteristics that differed from a typical supercell observed in a dry environment. They also suggested that a significant fraction of tornadic storms in Japan are mini supercells. Using dual-Doppler analysis and numerical simulations, Shimizu et al. (2008) described a structure and formation mechanism for a "supercell-like storm" in a moist environment. There have been several detailed studies of supercell storms and tornadoes in the United States based on high-resolution observational data obtained using mobile Doppler radars (e.g., Wurman et al. 1997, 2002; Markowski et al. 2012a,b). However, there have been few such studies in Japan that have observed both a

mesocyclone and a tornado simultaneously using Doppler radars.

The purpose of the present study is to describe the relationship between the tornado vortex and the mesocyclone, as well as their vertical profiles, within the Fukuoka tornado. Fortunately, the C-band Doppler radar of the Japan Meteorological Agency (the JMA radar) and several X-band polarimetric radars are situated near Fukuoka, and they detected the mesocyclone and precipitation pattern within the parent storm. In addition, the tornado vortex was observed by the C-band Doppler radar at Fukuoka airport (DRAW: Doppler Radar for Airport Weather), located about 2 km from the damage track of the Fukuoka tornado. In this paper, we present our analysis of the data obtained from these radars.

## 2. INSTRUMENTATION AND DATA ANALYSIS

Six Doppler radar stations are available across Fukuoka Prefecture, Japan (Fig. 1a). To analyze the characteristics of the tornado vortex and mesocyclone, plan position indicator (PPI) datasets from the JMA radar and DRAW were used in this study. In addition, constant altitude PPI (CAPPI) datasets from the X-band Doppler radars were used to investigate the morphology of the parent storm echo. A video of the Fukuoka tornado, which was taken around 0641 Japan Standard Time (JST, = UTC + 9 hours), was also used. The video was taken facing south, from a location about 1 km north of the Fukuoka tornado (Fig. 1b).

### 2.1 Radar Observations

The JMA radar has a maximum observation range of 240 km and is located on the border between Fukuoka and Saga prefectures (Fig. 1a). The sampling resolution of the JMA radar data is 500 m in the radial direction and 1.0° in azimuth. One volume scan consists of 26 elevation angles and takes 10 minutes. Low elevation angle PPI scans (EL = -0.3°, 1.2°, 2.8°, and 4.5°), providing both the reflectivity and Doppler velocity data, are also taken every 5 minutes. The DRAW system has

---

\* Corresponding author address: Tetsuya Kobayashi, Hydrospheric Atmospheric Research Center, Nagoya University, Nagoya 464-8601, Japan; email: tetsuk@rain.hyarc.nagoya-u.ac.jp

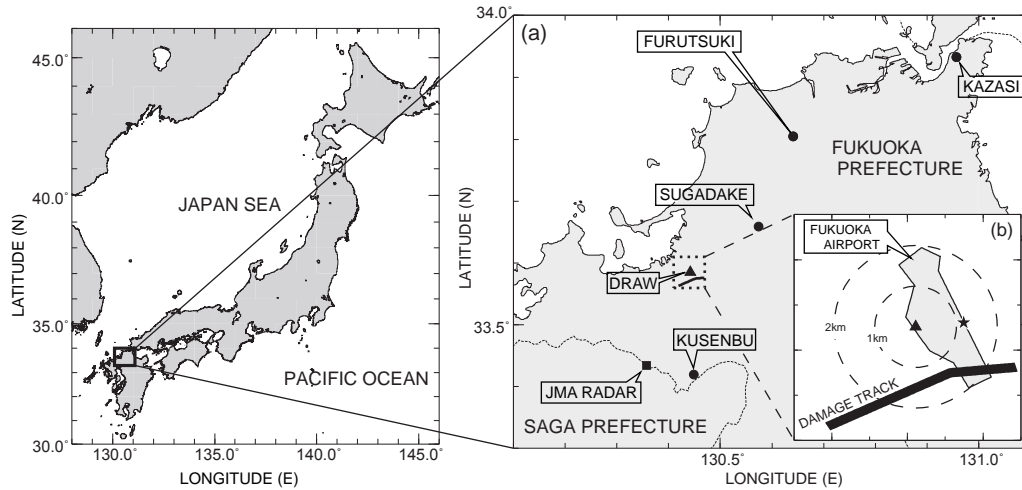


FIG. 1. Maps of (a) locations of radars and (b) the Fukuoka airport area. In both maps, the damage track is indicated by the black solid line, and the DRAW of the Fukuoka airport is indicated by the solid triangle. (a) Solid circles show the location of MLIT radars located at Kazasi, Furutsuki, Kusenbu and Sugadake. The solid square shows the location of the JMA radar. The dashed square is the region of (b). (b) Dashed range circles represent observational range of the DRAW at 1-km and 2-km. The star indicates the location of the videophotographing. The shaded area indicates the Fukuoka airport.

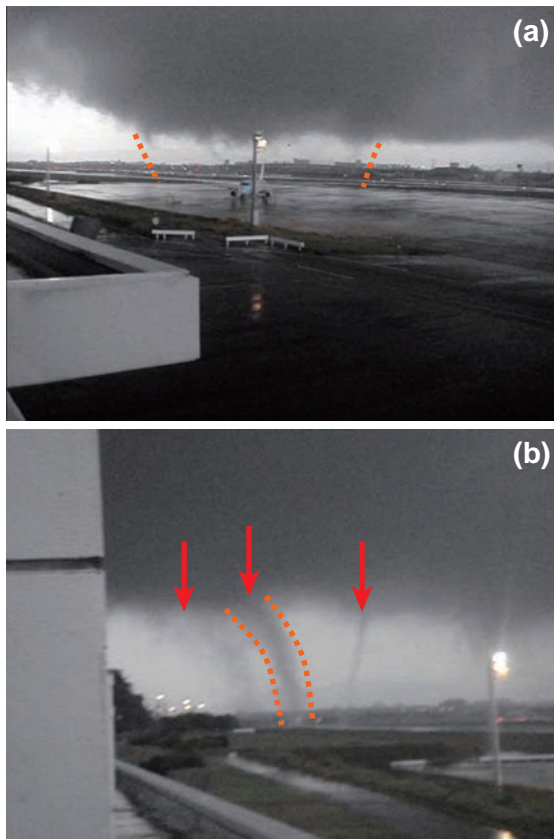


FIG. 2. Two snapshots, (a) and (b), from the video of the Fukuoka tornado. Suction vortices are indicated by arrows in (b). In (a), dash lines show outline of the tornado. In (b), dash lines show outline of one of suction vortices. The view is to the south from a location approximately 1-km north of the tornado. (Courtesy of the Fukuoka airport office.)

a maximum observation range of 120 km and is located at Fukuoka airport (Fig. 1b). The sampling resolution of the DRAW data is 150 m in the radial direction and  $0.7^\circ$  in azimuth. One volume scan consists of 20 elevation angles and takes 6 minutes. Low elevation angle PPI scans ( $0.7^\circ$  and  $2.1^\circ$ ) are taken approximately every minute.

We used the four X-band polarimetric radars of the Ministry of Land, Infrastructure, Transport and Tourism (MLIT radar) located at Kazashi, Furutsuki, Kusenbu, and Sugadake in Fukuoka Prefecture, Japan (Fig. 1a) to observe the echo above the DRAW system and to obtain low-level observational datasets over a wide area. The maximum observation range of the MLIT radar is 80 km, and the sampling resolution is 150 m in the radial direction and  $1.2^\circ$  in azimuth. One volume scan consists of 12 elevations and takes 5 minutes.

The MLIT radar data were interpolated onto a Cartesian coordinate system (CAPPI dataset), with a grid spacing of  $0.5 \times 0.25$  km (horizontal  $\times$  vertical). We used CAPPI datasets at 1 km above sea level (ASL) to exclude the influence of ground clutter, and employed a Cressman-type weighting function for the interpolation.

## 2.2 Vortex detection

Using the PPI scan datasets, the mesoscale vortex was detected manually using the following identification criteria (Donaldson 1970; Suzuki et al. 2000):

1) a pair of maximum and minimum Doppler velocities was detected on at least two adjacent

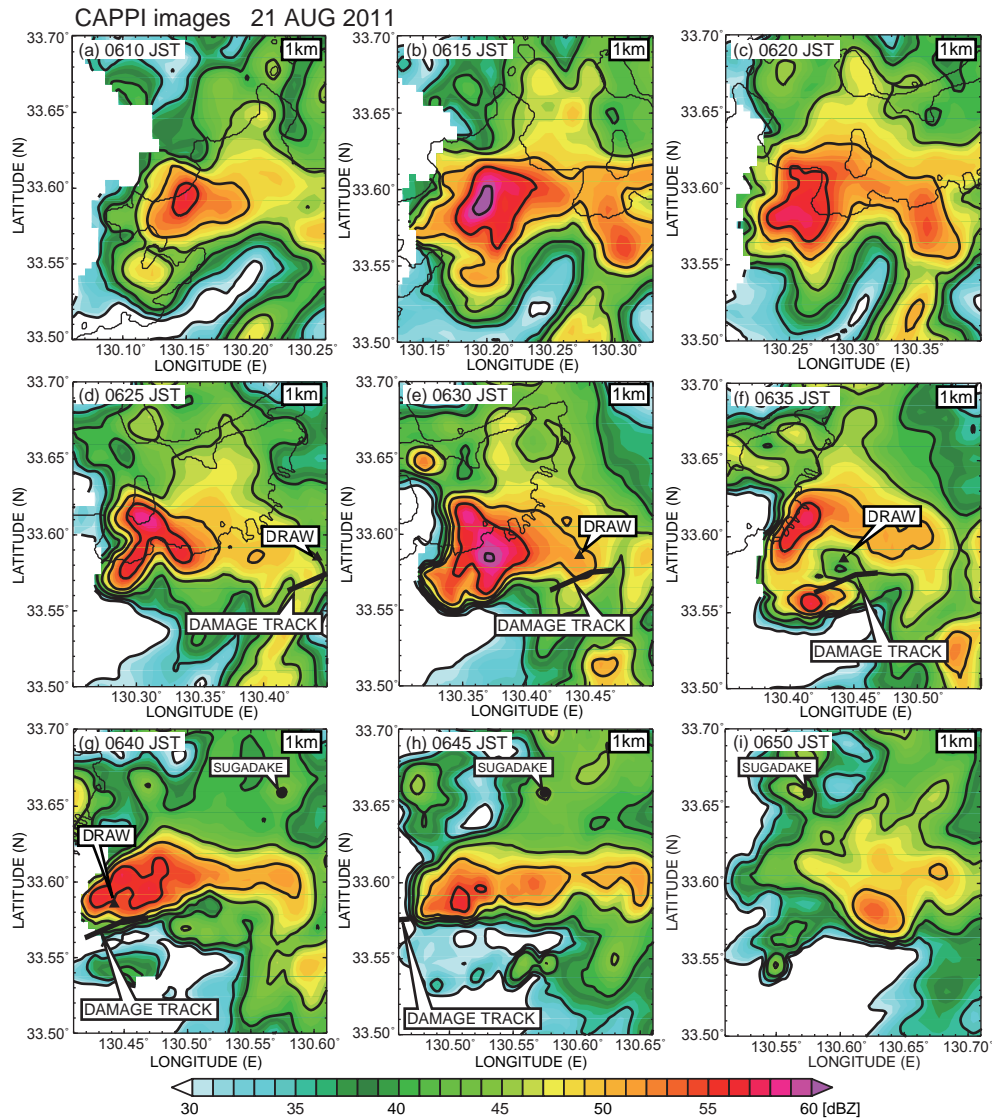


FIG. 3. (a)-(i) Horizontal distribution of the reflectivity at 1 km ASL from 0610 to 0650 JST. The contours indicate the reflectivity every 5 dBZ from 30 to 60 dBZ. The thick solid line indicates the damage track. The solid triangle and solid circle indicate locations of the DRAW and MLIT radar (Sugadake), respectively.

elevation angles and two successive scans;

2) the angle between the beam direction and the line segment connecting the maximum and minimum points of Doppler velocity was more than  $45^\circ$ ;

3) the vertical vorticity was greater than  $1.0 \times 10^{-2} \text{ s}^{-1}$ , where the vertical vorticity was calculated by dividing half of the difference between the maximum and minimum Doppler velocities by the vortex diameter. The vortex diameter was estimated as the distance between a pair of maximum and minimum points of Doppler velocity.

The mesoscale vortex is generally classified as either a mesocyclone or misocyclone based on its diameter (Fujita 1981), the criterion being 4 km. However, in this paper, we refer to the vortex of the

parent storm as the “mesocyclone” (MC), regardless of its diameter (after Suzuki et al. 2000), while the smaller-scale vortex embedded within the MC is referred to as a “misocyclone” (mc).

### 3. OVERVIEW OF THE FUKUOKA TORNADO AND THE PARENT STORM

The locations of the Fukuoka tornado and the damage track surveyed by JMA are shown in Fig. 1. The intermittent damage length was about 5 km and the damage width was about 150 m. The Fukuoka tornado occurred at about 0638 JST on 21 August 2011. It moved east-northeastwards and turned east at the western end of Fukuoka airport. Its lifespan was about six minutes. As shown in

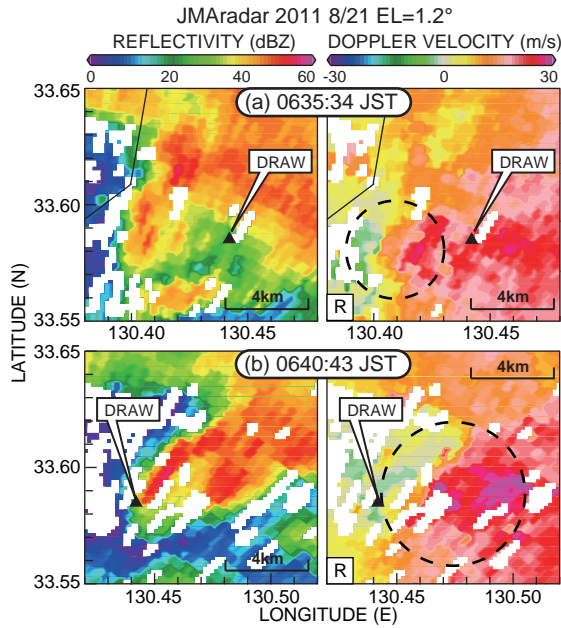


FIG. 4. PPI scan images of (left) reflectivity and (right) Doppler velocity fields at an elevation angle  $1.2^\circ$  at (a) 0635:34 JST and (b) 0640:43 JST 21 August 2011 as measured by the JMA radar. In the Doppler velocity fields, dashed circles delimit the region of the MC. Direction of radar site is indicated by "R". The DRAW of the Fukuoka airport is indicated by the solid triangle.

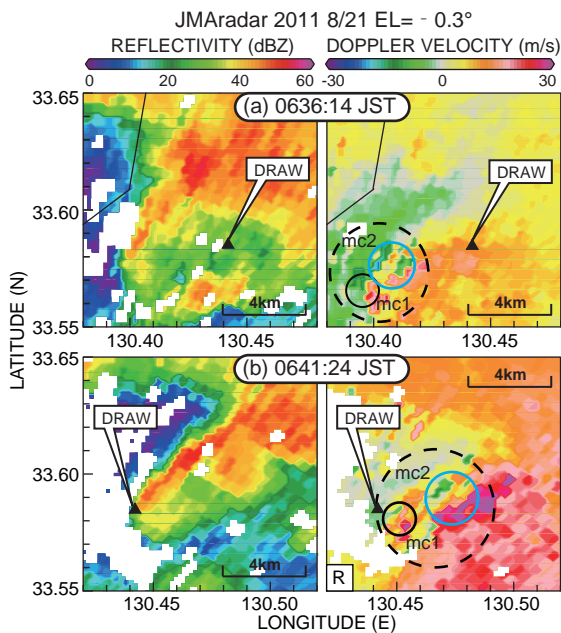


FIG. 5. PPI scan images of (left) reflectivity and (right) Doppler velocity fields at an elevation angle  $-0.3^\circ$  at (a) 0636:14 JST and (b) 0641:24 JST 21 August 2011 as measured by the JMA radar. In the Doppler velocity fields, dashed circles delimit the region of the MC. Small scale vortices, labeled "mc1" and "mc2", are indicated by black circle and blue circle, respectively. Direction of radar site is indicated by "R". The DRAW of the Fukuoka airport is indicated by the solid triangle.

Fig. 1b, at the end of its lifespan, the tornado crossed the southern edge of Fukuoka airport and left debris on a runway.

The sounding data from Fukuoka city show that a strong vertical shear, accompanied by veering and a low-level moist layer, had developed by 0900 JST (not shown). The lifted convection level (LCL), corresponding to the cloud base, was at 938.9 hPa, the convective available potential energy (CAPE) was  $796.5 \text{ J kg}^{-1}$ , and the storm's relative helicity (SReH) was  $252.8 \text{ m}^2 \text{ s}^{-2}$ . The value of SReH is higher than the threshold value ( $150 \text{ m}^2 \text{ s}^{-2}$ ) for mesocyclone formation noted by Davis-Jones et al. (1990).

Figure 2 presents two snapshots from the video of the Fukuoka tornado, from which the height of the cloud base and the width of the Fukuoka tornado were estimated to be about 80 m and 400 m, respectively (Fig. 2a). These observations suggest that this tornado had a very large diameter, and also that the base height of its parent cloud was very low. Despite being rated as F1 on the Fujita scale, the Fukuoka tornado showed a multiple-vortex structure, which contained more than three simultaneous suction vortices, as seen in Fig. 2b (Fujita 1981). In Japan, this was the fourth observational case of a multiple-vortex tornado at that time. Last year, the fifth case, the Tsukuba tornado, was observed and described by Yamauchi et al. (2013). Suction vortices, of which the diameter was estimated to be 10–20 m near the surface, repeatedly appeared and dissipated. Although the outline of the Fukuoka tornado could not be described as a funnel cloud, we classified it as a mortar-like shape based on the outward inclination of these suction vortices. Some of the suction vortices curved towards the opposite direction to the tornado's rotation in the upper part.

The evolution of the parent storm at 1 km ASL from 0610 to 0650 JST is shown in Fig. 3. This figure is based on the CAPPI datasets from the four MLIT radars. Before 0610 JST, the echo showed a quasi-linear pattern aligned in an east–west direction (not shown here). A hook echo structure ( $\geq 40 \text{ dBZ}$ ) was seen in the parent storm from 0610 to 0635 JST (Fig. 3a–f). From 0625 to 0645 JST, there was a large reflectivity gradient in the western section of this storm, and the high reflectivity echo region of  $>30 \text{ dBZ}$  extended eastwards (Fig. 3d–h). At 0615 and 0630 JST, the reflectivity exceeded 60 dBZ (Fig. 3b, e). After each peak echo appeared, a significant hook echo structure, which was characterized by an echo region greater than 45 dBZ, appeared in the southwest of the parent storm (Fig. 3d, f). At 0625 JST, as shown in Fig. 3d, the first significant hook echo structure was connected to the strong echo region ( $\geq 50 \text{ dBZ}$ ) in the parent storm. On the other hand, the second was

separated into two strong echo regions ( $\geq 50$  dBZ) at 0635 JST, which were located in the west and southwest sectors of the parent storm (Fig. 3f). In addition, a bounded weak echo region (BWER; Lemon and Doswell 1979) was observed in the center of the hook echo structure at 0635 JST. The strong echo region ( $\geq 50$  dBZ) located in the southwest area of this storm decayed gradually from 0635 to 0645 JST. The Fukuoka tornado developed after the appearance of the second significant hook echo structure (which had the two strong echo regions). As the parent storm passed over the damage track from 0635 to 0645 JST, the Fukuoka tornado was located at the head of the hook echo structure and to the southwest of the parent storm. After 0650 JST, the storm moved eastward and decayed gradually.

#### 4. STRUCTURE OF THE MESOCYCLONE AND THE FUKUOKA TORNADO

##### 4.1 Analysis of the JMA radar data

Figure 4 shows PPI scan images of reflectivity and Doppler velocity fields at an elevation angle of  $1.2^\circ$  ( $EL = 1.2^\circ$ ) from 0635 to 0640 JST as measured by the JMA radar. Figure 5 is the same as Fig. 4, but at an elevation angle of  $-0.3^\circ$  ( $EL = -0.3^\circ$ ) from 0636 to 0641 JST. At both elevation angles, a hook echo structure is apparent in the reflectivity fields. At  $EL = 1.2^\circ$ , there was a pair of maximum and minimum Doppler velocities near the hook echo region (about 1500 m ASL), indicated by dashed circles in the Doppler velocity fields (Fig. 4). As this pair of Doppler velocities satisfied the identification criteria (see section 2.2), we classified them as a counterclockwise MC. At 0635:34 JST (0640:43 JST), the maximum Doppler velocity ( $V_{max}$ ) was  $28 \text{ m s}^{-1}$  ( $32 \text{ m s}^{-1}$ ) and the minimum ( $V_{min}$ ) was  $-16 \text{ m s}^{-1}$  ( $-4 \text{ m s}^{-1}$ ). The vortex diameter was 3.1 km (5.7 km) and the vorticity was  $0.028 \text{ s}^{-1}$  ( $0.013 \text{ s}^{-1}$ ) at  $EL = 1.2^\circ$  at 0635:34 JST (0640:43 JST). The MC was detected near the western edge of the strong echo region from  $EL = -0.3^\circ$  to  $EL = 6.5^\circ$  (from about 900 to 4000 m ASL). At  $EL = -0.3^\circ$ ,  $V_{max}$  was  $28 \text{ m s}^{-1}$  ( $32 \text{ m s}^{-1}$ ) and  $V_{min}$  was  $-10 \text{ m s}^{-1}$  ( $-2 \text{ m s}^{-1}$ ) at 0636:14 JST (0641:24 JST). The diameter of the MC at  $EL = -0.3^\circ$  was 4.3 km (5.2 km) at 0636:14 JST (0641:24 JST). In the Doppler velocity field at  $EL = -0.3^\circ$ , two other pairs of maximum and minimum Doppler velocity showing counterclockwise rotation were detected at about 900 m ASL within the circulation of the MC from 0636 to 0646 JST, and they were misocyclones that were smaller than the MC. One of these two misocyclones was located in the southwestern region of the MC at  $EL = 1.2^\circ$  (mc1: indicated by black circles in Fig. 5). The diameter of

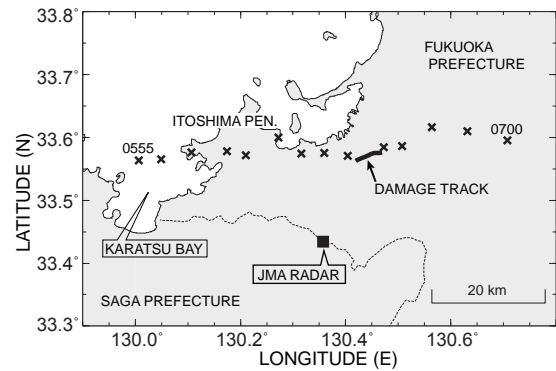


FIG. 6. The track of the mesocyclone (MC) detected by the JMA radar at an elevation angle  $1.2^\circ$  on 21 August 2011. The crosses show the location of MC. The JMA radar is indicated by a solid square. The damage track is indicated by a thick line.

mc1 was about 900 m. The other misocyclone, mc2, was located near the center of the MC at  $EL = 1.2^\circ$ , which is indicated by blue circles in Fig. 5. The diameter of mc2 was approximately 1.2 km. The diameters of mc1 and mc2 changed little from 0636 to 0646 JST (not shown).

The track of the MC detected by the JMA radar at  $EL = 1.2^\circ$  is shown in Fig. 6. The MC was first detected over Karatsu Bay at 0555 JST, and then moved eastward before turning inland and crossing the Itoshima Peninsula at about 0605 JST. The MC passed close to the damage track of the Fukuoka tornado between 0635 and 0645 JST. As the Fukuoka tornado occurred at around 0638 JST, these observations suggest that it was produced by the system accompanied by the MC that persisted for about 65 minutes.

The characteristics of the parent storm of the Fukuoka tornado analyzed by the JMA radar and MLIT radars, such as the hook echo structure and long-lived MC, suggest that the parent storm was similar to a typical supercell storm with a mesocyclone.

##### 4.2 Analysis of the DRAW data

Figure 7 shows PPI scan images of reflectivity and Doppler velocity fields at  $EL = 2.1^\circ$  from 0637 to 0641 JST, derived from DRAW data. At 0637 JST and 0641 JST, a hook echo structure can be seen in the reflectivity fields. At 0641 JST, a circular missing-echo region had developed within the hook echo (Fig. 7b). This region, at  $EL = 2.1^\circ$  (about 100 m ASL), was observed from 0638 to 0644 JST, and this is consistent with the occurrence of the Fukuoka tornado. The diameter of this circular region was about 500 m at  $EL = 2.1^\circ$ , which corresponds to the diameter (about 400 m) of the

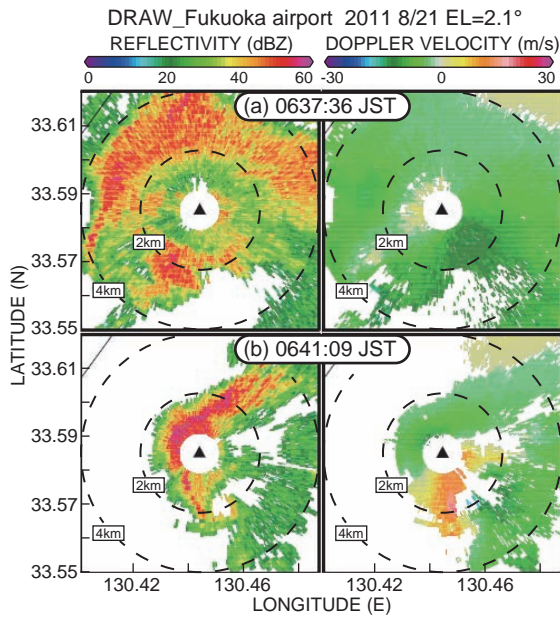


FIG. 7. PPI scan images of (left) reflectivity and (right) Doppler velocity fields at an elevation angle  $2.1^\circ$  at (a) 0637:36 JST and (b) 0641:09 JST 21 August 2011 as measured by the DRAW. The location of the radar is indicated by a solid triangle. Dashed range circles represent observational range of the DRAW at 2-km and 4-km.

Fukuoka tornado at the height of the cloud base (about 80 m ASL), as estimated from the video footage. The Doppler velocity field around the circular missing-echo region showed a counterclockwise vortex pattern. We consider that this Doppler velocity field indicates the low-level rotation of the Fukuoka tornado. Thus, the circular region of missing data at the edge of the hook echo structure directly represents the core diameter of the tornado vortex. The circular missing-echo region was observed from  $EL = 2.1^\circ$  to  $EL = 4.1^\circ$  (about 170 m ASL). In the Doppler velocity field, the tornado vortex was observed up to  $EL = 27.7^\circ$  (about 750 m ASL). We propose that the missing echo was caused by the exclusion of data during quality control due to wind perturbation by suction vortices smaller than the radar resolution and by the absence of large-diameter raindrops acting as scatterers in the tornado vortex.

#### 4.3 Relationship between the MC and the tornado

Figure 8 shows the locations of the tornado vortex and the MC around the occurrence time of the Fukuoka tornado. The location of the tornado vortex generally corresponded to the damage track of the Fukuoka tornado. The tornado vortex was also located in the southeastern quadrant of

rotation of the MC. The center of the MC was located in front of the tornado vortex at each elevation.

To generate vertical profiles of the MC, mc1, mc2, and tornado vortex, we estimated the positions of each vortex at 0640:43 JST. The diameter and position of the tornado vortex were obtained from the missing-echo region at  $EL = 2.1^\circ$  and  $4.1^\circ$ , and from the Doppler velocity field at the other elevation angles. Figure 9 shows vertical profiles across north–south and east–west sections at 0640:43 JST. In this figure, the horizontal axis indicates gaps at the center of vortices in the north–south and east–west directions from the center of the MC that was observed on the JMA radar at  $EL = 1.2^\circ$  at 0640:43 JST. The diameters of the other elevations of the JMA and DRAW radars were estimated using the scan from the nearest time to 0640:43 JST. On S–N and W–E cross-section, the diameters of the MC and the tornado vortex were relatively constant in a vertical sense, respectively. In contrast, there was a large difference in the diameters of the MC and the mesocyclones around 0640 JST.

The tornado vortex was approximately 1.5 km south and 2.5 km west (or approximate 3 km southwest) of the center axis of the MC. The position and diameter of mc1, located on the southwestern side of the MC, correspond to those of the low-level tornado vortex observed by DRAW. The mc2 was located close to the center of the MC. We suggest that mc1, observed by the JMA radar, played some part in connecting the tornado vortex near the surface to the MC within the parent storm. However, a low-level vortex that was connected to the MC through mc2 was not observed by DRAW. Although there was little tilting of the tornado vortex,

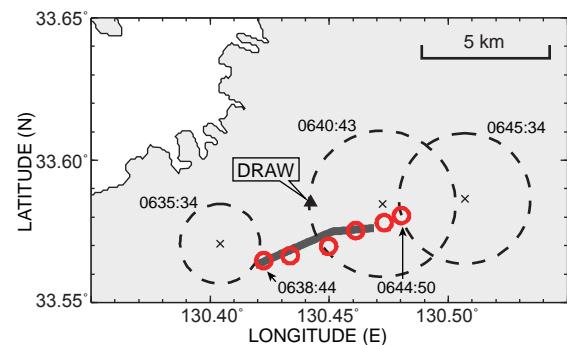


FIG. 8. The locations of the MC and the tornado vortex from 0635 JST to 0645 JST 21 August 2011. Red circles show a diameter of the tornado vortex detected by the DRAW, indicated by a solid triangle, at an elevation angle  $2.1^\circ$ . Crosses show the center of the MC detected by the JMA radar at an elevation angle  $1.2^\circ$ . Numerals by circles show the time of the detection of the MC and the tornado vortex. The damage track is indicated by a thick line.

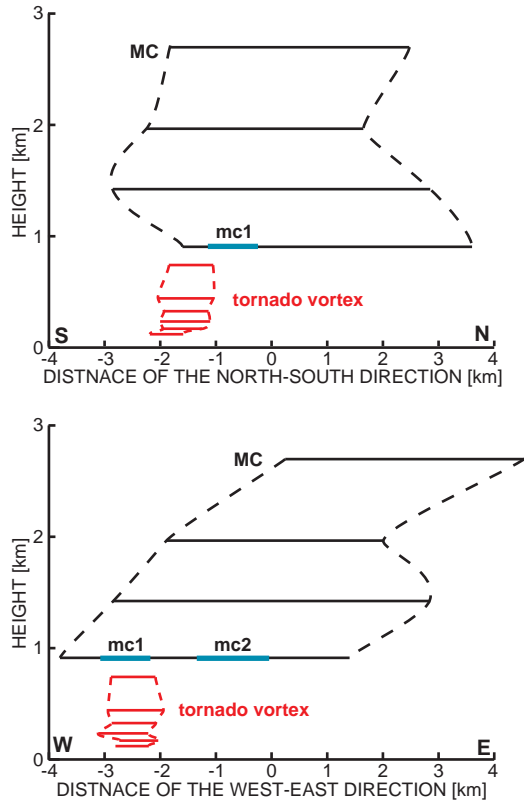


FIG. 9. Vertical profiles of the diameter of the MC (black solid lines), mc1 and mc2 (blue solid lines), the tornado vortex (red solid lines) across (top) the north - south and (bottom) west - east section at 0640:43 JST. The zero point is the center of the MC at an elevation angle  $1.2^\circ$  at 0640:43 JST. Black and red dashed lines show the outlines of the MC and the tornado vortex, respectively.

the MC tilted toward the northeast, which corresponds to the movement direction of the parent storm.

## 5. CONCLUSIONS

The parent storm of the Fukuoka tornado showed a hook echo similar to a typical supercell. Two significant hook echoes appeared successively in the precipitation system observed by the MLIT radars. In particular, the second hook echo separated into two strong echo regions ( $\geq 50$  dBZ) at 0635 JST, which may correspond to the forward flank downdraft and rear flank downdraft. The Fukuoka tornado occurred about 4 minutes after the appearance of this significant hook echo.

We detected a mesocyclone near the western edge of the strong echo region in the JMA radar data. The MC persisted for more than 1 hour. The MC moved east and passed close to the damage track between 0635 and 0645 JST. Consequently, we suggest that the Fukuoka tornado originated from a supercell storm containing a mesocyclone.

From 0636 JST, the JMA radar detected two counterclockwise misocyclones within the mesocyclone at an elevation angle of  $-0.3^\circ$ . At almost the same time, the hook echo structure with the vortex was also observed by DRAW. Although the Fukuoka tornado showed a multiple-vortex structure, the diameter of the suction vortices was less than the resolution of DRAW. Subsequently, the circular missing-echo region was observed within a head of the hook echo. As the diameter of missing-echo regions was almost the same as that of the Fukuoka tornado (observed visually), we believe that the circular missing-echo region indicates the core of the Fukuoka tornado. Both the diameters of the MC and the tornado vortex were relatively constant in a vertical sense, respectively. The tornado vortex was located about 3 km southwest of the center of the MC in the PPI data at an elevation angle of  $1.2^\circ$ . The MC became inclined eastward, whereas the tornado vortex remained a vertical column. We suggest that the tornado vortex connected vertically to the misocyclone; the diameter and position of the tornado vortex corresponded to those of one of two misocyclones (referred as "mc1" in this study) embedded in the MC.

*Acknowledgments.* This study was supported in part by The Japan Society for the Promotion of Science (JSPS), KAKENHI Grant Number 22310112. Radar data of the Japan Meteorological Agency were obtained from the National Institute of Information and Communications Technology (NICT) archive, and the Doppler radar for airport weather (DRAW) data were provided by the Fukuoka aviation weather station. The video images were provided by the Fukuoka airport office of the Land, Infrastructure and Transportation Ministry of Japan. The authors also thank the Ministry of Land, Infrastructure, Transport and Tourism for providing data from their X-band polarimetric radar to the Research Consortium on Technological Development of MLIT's X-band Multi-parameter Radar.

## REFERENCES

- Davies-Jones, R. P., D. Burgess, and M. Foster, 1990: Test of helicity as a tornado forecast parameter. Preprints, 16th Conf. on Severe Local Storms, Kananaskis Park, AB, Canada, Amer. Meteor. Soc., 588-592.
- Donaldson, R. J., Jr., 1970: Vortex signature recognition by a Doppler radar. *J. Atmos. Sci.*, 9, 661-670.
- Fujita, T. T., 1981: Tornadoes and downbursts in the context of generalized planetary scales. *J. Atmos. Sci.*, 38, 1511-1534.

- Inoue, Y. H., K. Kusunoki, W. Kato, H. Suzuki, T. Imai, T. Takemi, K. Bessho, M. Nakazato, S. Hoshino, W. Mashiko, S. Hayashi, T. Fukuhara, T. Shibata, H. Yamauchi, and O. Suzuki, 2011: Finescale Doppler Radar Observation of a Tornado and Low-Level Mesocyclones within a Winter Storm in the Japan Sea Coastal Region. *Mon. Wea. Rev.*, 139, 351-369.
- Kobayashi, F., K. Kikuchi, and H. Uyeda, 1996: Life cycle of the Chitose tornado of September 22, 1988. *J. Meteor. Soc. Japan*, 74, 125-140.
- Lemon, L. R., and C. A. Doswell, 1979: Severe thunderstorm evolution and mesocyclone structure as related to tornadogenesis. *Mon. Wea. Rev.*, 107, 1184-1197.
- Markowski, P., Y. Richardson, J. Marquis, J. Wurman, K. Kosiba, P. Robinson, D. Dowell, E. Rasmussen, and R. Davies-Jones, 2012a: The Pretornadic Phase of the Goshen County, Wyoming, Supercell of 5 June 2009 Intercepted by VORTEX2. Part I: Evolution of Kinematic and Surface Thermodynamic Fields. *Mon. Wea. Rev.*, 140, 2887-2915.
- , ——, ——, R. Davies-Jones, J. Wurman, K. Kosiba, P. Robinson, E. Rasmussen, and D. Dowell, 2012b: The Pretornadic Phase of the Goshen County, Wyoming, Supercell of 5 June 2009 Intercepted by VORTEX2. Part II: Intensification of Low-Level Rotation. *Mon. Wea. Rev.*, 140, 2916-2938.
- McCaul, E. W., Jr., 1987: Observations of the Hurricane "Danny" tornado outbreak of 16 August 1985. *Mon. Wea. Rev.*, 115, 1206-1223.
- Niino, H., O. Suzuki, H. Nirasawa, T. Fujitani, H. Ohno, I. Takayabu, N. Kinoshita, and Y. Ogura, 1993: Tornadoes in Chiba prefecture on 11 December 1990. *Mon. Wea. Rev.*, 121, 3001-3018.
- , T. Fujitani, and N. Watanabe, 1997: A statistical study of tornadoes and waterspouts in Japan from 1961 to 1993. *J. Climate*, 10, 1730-1752.
- Simizu, S., H. Uyeda, Q. Moteki, T. Maesaka, Y. TAKAYA, K. AKAEDA, T. KATO, and M. Yoshida, 2008: Structure and Formation Mechanism on the 24 May 2000 Supercell-Like Storm Developing in a Moist Environment over the Kanto Plain, Japan. *Mon. Wea. Rev.*, 136, 2389-2407.
- Suzuki, O., H. Niino, H. Ohno, and H. Nirasawa, 2000: Tornadoproducing mini supercells associated with Typhoon 9019. *Mon. Wea. Rev.*, 128, 1868-1882.
- Wurman, J., 2001: The DOW mobile multiple-Doppler network. Preprints, 30th Int. Conf. on Radar Meteorology, Munich, Germany, Amer. Meteor. Soc., CD-ROM, P3.3.
- , 2002: The multiple-vortex structure of a tornado. *Wea. Forecasting*, 17, 473-505.
- , J. M. Straka, E. N. Rasmussen, M. Randall, and A. Zahrai, 1997: Design and deployment of a portable, pencil-beam, pulsed, 3-cm Doppler radar. *J. Atmos. Oceanic Technol.*, 14, 1502-1512.
- Yamauchi, H., H. Niino, O. Suzuki, Y. Shoji., E. Sato, A. Adachi, and W. Mashiko, 2013: Vertical structure of the Tsukuba F3 tornado on 6 May 2012 as revealed by a polarimetric radar. 36th Conf. on Radar Meteorology, Breckenridge, CO, Amer. Meteor. Soc., 320.